HHS Public Access

Author manuscript

Ann N Y Acad Sci. Author manuscript; available in PMC 2018 October 01.

Published in final edited form as:

Ann N Y Acad Sci. 2017 October ; 1405(1): 116–130. doi:10.1111/nyas.13439.

T cell protein tyrosine phosphatase prevents STAT1 induction of claudin-2 expression in intestinal epithelial cells

Moorthy Krishnan and **Declan F. McCole**

Division of Biomedical Sciences, University of California, Riverside, California

Abstract

T cell protein tyrosine phosphatase (TCPTP) dephosphorylates a number of substrates, including JAK–STAT signaling proteins, which are activated by interferon (IFN)-γ, a major proinflammatory cytokine involved in conditions such as inflammatory bowel disease (IBD). A critical function of the intestinal epithelium is formation of a selective barrier to luminal contents. The structural units of the epithelium that regulate barrier function are the tight junctions (TJs), and the protein composition of the TJ determines the tightness of the barrier. Claudin-2 is a TJ protein that increases permeability to cations and reduces transepithelial electrical resistance (TER). We previously showed that transient knockdown of TCPTP permits increased expression of claudin-2 by IFN-γ. Here, we demonstrate that the decreased TER in TCPTP-deficient epithelial cells is alleviated by STAT1 knockdown. Moreover, increased claudin-2 in TCPTP-deficient cells requires enhanced STAT1 activation and STAT1 binding to the *CLDN2* promoter. We also show that mutation of this STAT-binding site prevents elevated *CLDN2* promoter activity in TCPTP-deficient epithelial cells. In summary, we demonstrate that TCPTP protects the intestinal epithelial barrier by restricting STAT-induced claudin-2 expression. This is a potential mechanism by which loss-of-function mutations in the gene encoding TCPTP may contribute to barrier defects in chronic intestinal inflammatory disease.

Keywords

tight junction; inflammatory bowel disease; barrier function; interferon-γ; protein tyrosine phosphatase

Introduction

The inflammatory bowel disease (IBD) candidate gene protein tyrosine phosphatase non-receptor type 2 (PTPN2) encodes the ubiquitously expressed T cell protein tyrosine phosphatase (TCPTP) protein.[1] TCPTP directly dephosphorylates a number of substrates involved in cytokine and growth factor signaling, including members of the signal transducer and activator of transcription (STAT) family of transcription factors.[2–4] We and others have

Address for correspondence: Declan F. McCole, Ph.D.; Division of Biomedical Sciences, University of California, Riverside, 307 School of Medicine Research Building, 900 University Avenue, Riverside, CA 92521. declan.mccole@ucr.edu.

Competing interests

D.F.M. has a 2016 ASPIRE-Pfizer IBD Research Award investigator-initiated research grant from Pfizer Inc. M.K. has no conflict of interest to disclose.

shown that TCPTP acts as a negative regulator of interferon-γ (IFN-γ) signaling, as knockdown of TCPTP permits increased activation of STAT1 and STAT3 in intestinal epithelial cells (IECs).[5–7] Since TCPTP dephosphorylates STAT proteins in the cytoplasm and upon their translocation to the nucleus, it therefore plays an important role in limiting the downstream signaling initiated by inflammatory cytokines, such as IFN-γ.[7–9] Loss-of-function mutations in the *PTPN2* locus are associated with IBD, celiac disease, and type 1 diabetes, conditions that are also associated with increased intestinal permeability early in disease.[10–17]

We have previously shown that transient loss of TCPTP expression by small interfering RNAs (siRNAs) in intestinal epithelial cells (IECs) predispose to a more severe barrier defect induced by the IBD cytokine IFN-γ.[18,19] Specifically, we observed reduced transepithelial electrical resistance (TER) and increased permeability to FITC–dextran but no evidence of apoptosis. This is in agreement with other studies indicating that induction of epithelial apoptosis by IFN-γ is not a major contributor to barrier dysfunction.[20,21] The barrier defects observed in our previous studies of IFN-γ treatment of transient TCPTP siRNA knockdown IECs were associated with altered membrane localization of the tight junction (TJ) regulatory protein Zonula occludens-1 (ZO-1) and increased expression of the cation-pore forming TJ protein claudin-2.[18,19] Claudin-2 is a molecule of clinical significance, as its expression is increased in IBD, and it is also associated with metastatic potential in colorectal cancer.[22–27] Increased claudin-2 in epithelial TJs makes them more permissive to passive paracellular flux of sodium ions.[28–30] In addition, claudin-2 has been described as having the properties of a water channel.[31,32] Thus, given its capacity to act as a high-conductance cation-permeable paracellular pore, we can appreciate how elevated claudin-2 could increase cation flux into the intestinal lumen and thus contribute to fluid loss consistent with diarrhea.[33]

We previously described a STAT-binding site in the *CLDN2* promoter.[18] The aim of this study was to determine whether stable knockdown of TCPTP in IECs leads to increased expression of claudin-2 through STAT-mediated transcriptional regulation. Our results demonstrate that loss of TCPTP expression in IECs promotes increased expression and membrane localization of claudin-2 following IFN-ć treatment, which occurs in a STAT1-dependent manner. We further show that STAT1 binds to the *CLDN2* promoter and that mutation of the STAT-binding site eliminates IFN-γ induction of claudin-2. These data have implications for our understanding of how TCPTP restricts IFN-γ signaling and how disease-associated loss-of-function mutations in the PTPN2 gene may exacerbate barrier defects in chronic inflammatory diseases of the intestines.

Methods

Materials

Human recombinant IFN-γ (Roche, Mannheim, Germany), monoclonal mouse anti-β-Actin (Sigma-Aldrich, St. Louis, MO), monoclonal mouse anti-TCPTP antibody CF-4, which detects the 45-kD and 48-kD isoforms (Millipore, Billerica, MA), anti-phospho-STAT1 (Tyr^{701}), anti-STAT1, (Cell Signaling Technologies, Danvers, MA), anti-claudin-2, anti-occludin, anti-CDX2, and anti-ZO-1 antibodies (Invitrogen, Waltham, MA) were obtained

from the sources noted. Millicell culture plate inserts were purchased from Millipore Corporation (Millipore, Bedford, MA). McCoy's 5A and DMEM media were purchased form Corning Inc., (Corning, NY). The ON-TARGET plus SMART pool siRNA and ON-TARGET plus Non-targeting pool were purchased from GE Dharmacon (Pittsburgh, PA). All other reagents were of analytical grade and acquired commercially.

Tissue culture

Human Caco2-bbe and HT-29 intestinal epithelial cells were grown in Dulbecco's modified Eagle's medium and McCoy's 5A medium, respectively (HyClone Laboratories Inc., Logan, UT) with 10% heat-inactivated fetal bovine serum and 1% glutamine and penicillin (100 U/mL)/streptomycin (100μg/mL) at 37 °C in 5% CO2. Cells were fed 3 times a week.

Stable shRNA PTPN2-deficient cell line generation

As previously described, control shRNA and shRNA against *PTPN2* (Sigma-Aldrich, St. Louis, MO) were transfected into HEK293T cells along with packaging vector (pR8.2) and ENV plasmid (pMDG.2) (gifts from Dr. R. Daniel Beauchamp, Vanderbilt University, Nashville, TN) using Effectene reagent (Qiagen, Valencia, CA).[34] After 18 h, the cells were washed, and fresh media was added to the cells for 48 h, after which the cell supernatant was collected and filtered through a 0.45-μM filter (Millipore, Billerica, MA). The filtered media was used to infect HT-29 and Caco-2bbe cells by mixing equal amounts of fresh media with polybrene (5 mg/mL). After 72–96 h of infection, cells were stably selected using puromycin (1 μg/mL). The stable cell lines were maintained with 500 ng/mL puromycin. *PTPN2* knockdown was confirmed by both RT-PCR and immunoblotting methods.

Small interfering RNA transfection

HT-29 control shRNA (Con-shRNA) and PTPN2-knockdown (PTPN2-KD) IECs were seeded (5×10^5 cells on six-well plates and 2×10^5 cells on glass coverslips) and grown overnight. The next day, STAT1 siRNA SMARTpool and Control siRNA SMARTpool (25nM final concentration) were transfected into HT-29 Con-shRNA and PTPN2-KD cells using the DharmaFECT reagent according to the manufacturer's instructions. After 24 h of transfection, the cells were treated with IFN-γ for another 24 hours. The cells were either lysed with RIPA for western blot analysis or fixed with either 4% PFA or 100% methanol for immunofluorescence studies.

RNA isolation, real-time PCR, and quantitative PCR

The control and PTPN2-KD cell lines were plated on six-well plates, and total RNA was extracted using TRIzol reagent according to the manufacturer's instructions. RNA purity and concentration were assessed by absorbance at 260 and 280 nm. One microgram of total RNA was taken, and cDNA was made using qScript cDNA SuperMix (Quanta Biosciences, Beverly, MA). Two microliters of 5×-diluted cDNA was amplified using gene-specific primers and GoTaq Green, 2× mix (Promega Madison, WI) (sequences listed in Table 1). For quantitative PCR, the cDNA was prepared as described earlier. The qPCR was performed using a PowerUp SYBR Green Master Mix (Applied Biosystems, Foster City, CA) and a CFX96 Touch™ Real-Time PCR Detection System (Bio-Rad, Hercules, CA),

with gene-specific primers under the following conditions: 95 °C for 3 min, followed by 40 cycles at 95 °C for 15s, 55 °C for 30s, and 72 °C for 30 seconds. Measurements were performed in triplicate; human GAPDH was used as an endogenous control. The real-time PCR data were analyzed by the comparative *C*T (Δ Δ CT) method, as previously described.[35]

Preparation of Triton X-100–soluble and –insoluble fractions

The control and PTPN2-KD cell lines were seeded (1×10^6) on a 10-cm dish and grown for 3 days, and preparation of Triton X-100–soluble and –insoluble fractions was performed as described in published protocols.[36] In brief, cells were washed with 1× phosphate-buffered saline (PBS) and scraped in cold PBS. The cells were spun down at 400 × *g* for 5 min, and the pellet was lysed with lysis buffer (10 mM HEPES, pH 7.2, 1% Triton X-100, 100 mM NaCl, 2 mM EDTA, with phosphatase and protease inhibitors) and incubated at 4 °C for 20 min, followed by centrifugation at 9600 × *g* for 20 minutes. The resulting supernatant was considered the soluble fraction. The pellet from the soluble fraction was dissolved by pipetting in pellet solubilization buffer (10 mM HEPES, pH 7.2, 1% SDS, 100 mM NaCl, 2 mM EDTA, with phosphatase and protease inhibitors), and the samples were sonicated (10-s off and 10-s on cycle) for 2 min and incubated at 4 °C for 20 min, followed by centrifugation at 16,200 × *g* for 20 minutes. The supernatant was considered the insoluble fraction. Protein concentration was determined by the bicinchoninic acid (BCA) method using the respective lysis buffer as a blank.

Western blotting (SDS-PAGE)

The control and KD cells were seeded on six-well plates. After experimental treatments, the cells were washed with PBS and lysed in RIPA buffer (50 mM Tris-Cl, pH 7.4, 150 mM NaCl, 1% NP-40, 0.5% sodium deoxycholate, 0.1% SDS, with protease and phosphatase inhibitors) for 10 min at 4 °C. The lysate was sonicated (10-s off and 10-s on cycle) for 2 min and centrifuged at 16200 × *g* for 10 minutes. The supernatant was transferred to a new tube, and protein concentration was determined by the BCA method using the Pierce BCA protein assay reagent (Pierce, Rockford, IL). A 20-μg total protein amount was suspended in 1% SDS sample buffer, heated for 10 min at 95 °C, resolved on a 6–12% SDS–PAGE gel, and transferred to a PVDF membrane (Millipore). The blots were blocked in 5% TBS-T (5% dry milk powder in Tris-buffered saline, 0.01% Tween-20) for 30 min, followed by incubation with primary antibody diluted in 1% TBS-T overnight at 4 °C. The blots were then washed five times for 5 min at room temperature with TBS-T (0.1% Tween-20), incubated with horseradish peroxidase–conjugated secondary antibodies (Jackson ImmunoResearch) for 1 h at room temperature, and washed five times for 5 min at room temperature with TBS-T (0.1% Tween-20). Specific labeling was detected by chemiluminescence reagent (Pierce) and exposure to X-ray film (Labscientific Inc, Livingston, NJ). Densitometric analysis of western blots was performed using Image J software (NIH).

Small interfering RNA transfection of polarized IEC monolayers

The HT-29 Con-shRNA and PTPN2-KD IECs were seeded (5×10^5 cells on 12-well Transwells in triplicate) and grown for 7 days. On day 8, the TER across control and KD cell

monolayers was assessed using a voltohmeter (WPI, Sarasota, FL) and companion electrodes (Millipore). This time point was considered the 0 h time point. The media was changed, and cells were transfected either with STAT1 siRNA SMARTpool or with control siRNA SMARTpool (25 nM final concentration) into HT-29 Con-shRNA and PTPN2-KD cells using the DharmaFECT reagent according to the manufacturer's instructions (sequences listed in Table 2). After 24 and 48 h of transfection, the TER was measured in triplicate in each insert, and the mean was calculated to represent that individual time point in that individual insert. Measurements were calculated in Ω.cm2 and expressed as percent change in TER over time.

Immunoprecipitation

The cells were washed twice with 1× PBS and lysed with lysis buffer (30 mM Tris-HCl, pH 7.5, 150 mM NaCl, 20 mM Mg acetate, and 1% 3-[(3-cholamidopropyl)dimethylammonio]-1- propanesulfonate (CHAPS)). After 30 min of incubation rotating end over end at 4 °C, the lysates were centrifuged at 16200 × *g* for 15 min at 4 °C to remove the cell debris. Samples were precleared using 100 μg of lysate protein with 50 μL of Dynabeads for 2 h at 4 °C. For immunoprecipitation, the anti-TCPTP antibody or nonspecific immunoglobulin G (IgG) was incubated with Dynabeads for 1 h at room temperature. The beads were washed twice with PBS, resuspended in 200 mM triethanolamine (pH 8.2), and incubated for 10 min at room temperature. The beads were cross-linked with 20 mM dimethyl pimelimidate dihydrochloride for 30 min at room temperature. The Dynabeads were washed with 50 mM Tris-HCl (pH 7.5) for 15 min and then three times with TBS. The washed Dynabeads were incubated with precleared lysates overnight. Beads were washed with lysis buffer three times and eluted with 1.5% SDS–PAGE sample buffer and incubation for 10 min at 70 °C. The supernatant was analyzed by SDS–PAGE as described earlier.

Chromatin immunoprecipitation assay

After 2 days of seeding, Con-shRNA and PTPN2-KD cells were treated with IFN-γ (1000 U/mL (100 ng/mL)) for 24 hours. Cells were then cross-linked with formaldehyde (1% final concentration) and incubated for 10 min at room temperature. The cells were quenched by addition of glycine to each plate to reach a final concentration of 125 mM and incubated for 5 minutes. The media was removed and washed (×2) with 10 mL of ice cold 1× PBS. The cells were incubated with 4 mL of ice cold 1× PBS with appropriate protease inhibitors, and cells were scraped and transferred to a 15-mL conical tube and spun at 750 ×*g* for 10 min at 4 °C. The cell pellet was resuspended in 1 mL of nuclear lysis buffer (50 mM Tris-HC (pH8), 10 mM EDTA, and 1% SDS). The samples were sonicated (10-s off, 10-s on cycle) for 2 mins and centrifuged at 16200 ×*g* for 15 minutes. The DNA concentration was measured, and 100 μg of pre-cleared chromatin was incubated with anti-STAT1 antibody or with rabbit IgG at 4 °C overnight. The magnetic beads were pelleted using the Magnetic Particle Concentrator (MPC) and washed in high-salt buffer (×4). The beads were washed twice with TB buffer and resuspended in 300 μL of elution buffer (50mm Tris-Cl, 10mM EDTA) with proteinase K (20 μg/μL) and then incubated for 2 h at 55 °C. The samples were cross-linked overnight at 65 °C. The samples were then centrifuged at 16,200 × *g* for 5 min

and resuspended in 50 μL of TE buffer. The 5 μl of purified DNA was taken and PCR was performed using *CLDN2* promoter–specific primers.

CLDN2 promoter luciferase reporter assay

The human *CLDN2* promoter (from −900 bp to +112 bp) gene construct was purchased from Integrated DNA Technologies (IDT) (Coralville, IA). The construct was cloned into the luciferase vector pGL3-Basic (Promega, Madison, WI) (restriction enzyme sites Nhe1 and KpnI, respectively), and the sequence of the product was confirmed by sequencing analyses. A single mutation of the STAT binding site was generated using forward primer 5′-CATCATCACCTTCCGGGAAAGCAGCCA-3′ and reverse primer 5′-GTGGCTGCTTTCCCGGAAGGTGATGATG-3′. A triple mutation was generated using forward primer 5′-CCACTGCCATCACCTTTCCCGAGAGCAGCCACC-3′ and reverse primer 5′-GGTGGCTGCTCTCGGGAAAGGTGATGATGGCAGTGG-3′. The mutations were confirmed by sequencing analysis. The cells were seeded onto 12-well plates in triplicate (technical replicates) and allowed to grow overnight to reach 50–60% confluence. The following day, cells were co-transfected with a firefly luciferase reporter construct and a reference construct that contains *Renilla reniformis* luciferase, phRL-TK (Promega, Madison, WI), using Effectene reagent (Qiagen). After 24-h transfection, the cells were treated with IFN-γ (1000 U/mL (100 ng/mL)). Twenty-four hours later, luciferase activities were measured using the Dual Luciferase Reporter Assay System kit (Promega) in a Glomax multi detection system (Promega). Firefly luciferase activity was normalized to *Renilla* luciferase activity and plotted as mean ± SEM from three independent experiments.

Immunofluorescence staining and quantification

HT-29–control and PTPN2-KD cell lines were plated on coverslips (12-well) and cultured for 3 days. After treatment, the cells were washed (×2) with PBS and fixed with either 100% methanol for 5 min at −20 °C or with 4% PFA for 20 min at room temperature. Cells were washed (×2) with PBS and permeabilized with 0.3% Triton X-100 in PBS for 30 min at room temperature. Cells washed (×2) with PBS and blocked with 10% normal donkey serum (Jackson ImmunoResearch) for 30 min at room temperature. Cells were incubated overnight at 4 °C with primary antibodies diluted in 1% normal donkey serum and 0.01% Tween-20 in PBS. The next day, cells were washed 5 times for 5 min at room temperature with 0.01% Tween-20 in PBS (PBS-T). The cells were incubated with appropriate secondary antibodies conjugated with Alexa Fluor 488 or Alexa Fluor 594 for 1 h at room temperature. At the end of the incubation, cells were washed (×5) with PBS-T and then washed in water and mounted with ProLong Gold plus DAPI (Invitrogen). All images were captured with a Leica DM5500 microscope attached to a DFC365 FX camera using a 63× oil immersion objective with an additional 2× digital zoom. The individual images were converted to tiff files with the LAS-AF lite software, and Photoshop (Adobe) was used to create the final figures. The total fluorescence measurements were performed with Image J software, and densitometric analysis was performed on 9–10 images from three different fields of view.

Statistical analysis

All data are means ± SEM for a series of experiments. Technical replicates are indicated in the specific description of the relevant method. The number of biological replicates is

indicated in the figure legend. Statistical analysis was performed by Student's unpaired *t*-test or analysis of variance (ANOVA) and Student–Newman–Keuls post-test using Graph Pad Instat 3 software (Graph Pad Software, La Jolla, CA). *P* values < 0.05 were considered significant.

Results

Stable knockdown of TCPTP causes increased claudin-2 expression in intestinal epithelial cell lines

We utilized two stable PTPN2-KD intestinal epithelial cell (IEC) lines generated using parental Caco-2bbe and HT-29 cells. Transfection of *PTPN2* shRNA reduced *PTPN2* mRNA compared with cells transfected with control shRNA or parental Caco-2bbe and HT-29 cells as determined by qPCR, thus confirming our previous data in HT-29 PTPN2-KD IECs (Fig. 1A and 1B).[34] Knockdown of *PTPN2* mRNA was specific, as mRNA of the closely related protein tyrosine phosphatase PTP1B was unaffected compared with control shRNA and parental HT-29 IECs (Fig. 1C). The mRNA levels of the PTPs SHP1 and SHP2 were also unaffected by PTPN2 shRNA (Fig. 1D and 1E). We previously demonstrated a reduction in TCPTP protein levels in PTPN2-KD IECs by probing whole-cell lysates. Here, we confirmed TCPTP knockdown by specifically immunoprecipitating TCPTP from cell lysates of Con-shRNA and PTPN2-KD HT-29 IECs and probing for TCPTP levels by crosslinking (Fig. 1F). Quantification of the resulting western blots confirmed significant knockdown of TCPTP protein equivalent to the reduction in mRNA levels (Fig. 1G). We previously reported that PTPN2-KD IECs exhibit reduced TER, even in the absence of inflammatory cytokine challenge.[34] The transmembrane protein claudin-2 forms a cation-selective pore in the apical tight junction that increases permeability to cations, such as sodium, and reduces TER.[29,30,33] To determine whether the previously described decrease in TER in PTPN2-KD IECs is associated with reduced transcription of claudin-2, we probed for CLDN2 mRNA levels by RT-PCR and qPCR. PTPN2-KD cells showed significantly increased CLDN2 mRNA compared with control and parental cells in both Caco-2bbe (Fig. 1. H and 1I) and HT-29 cell lines (Fig. 1J).

Increased STAT1 phosphorylation in PTPN2-KD IECs mediates IFN-γ-stimulated claudin-2 protein expression

Confirmation that claudin-2 protein expression was increased in PTPN2-KD cells (HT-29) was provided by western blotting, which showed reduced TCPTP correlated with significantly increased claudin-2 levels in both the cytosol (Triton-X–soluble) and, as expected, in the cell membrane (Triton-X–insoluble) fractions of cell lysates (Fig. 2A and 2B). In support of these data and in agreement with earlier findings, immunofluorescence staining identified increased claudin-2 levels in cell–cell junctions in PTPN2-KD HT-29 IECs (Fig. 2C).[29,30,34]

STAT1 is a key mediator of cytokine signaling pathways and is a prominent substrate of TCPTP. Dephosphorylation of STAT1 on its key activating tyrosine residue (Y701) reduces its transcriptional activity. TCPTP can dephosphorylate STAT1 in the cytoplasm and the nucleus and thus plays an essential role in restricting STAT1-mediated signaling and

transcription.[5,7] We previously observed that transient knockdown of TCPTP by siRNA permits increased STAT1 phosphorylation by IFN-γ and that the *CLDN2* promoter contains a STAT-binding site.[18] Here, we investigated whether this was recapitulated in stable PTPN2-KD IECs and whether the elevation in STAT1 was responsible for the increase in claudin-2 in these cells. Control shRNA and PTPN2-KD HT-29 IECs were transfected with control (scrambled) siRNA or STAT1 siRNA. STAT1 (Y701) phosphorylation, STAT1 expression, and claudin-2 expression were determined in these transfected cells with or without IFN-γ treatment for 24 h (1000 U/mL (100 ng/mL)).[18,19,37] STAT1 phosphorylation was increased in untreated and IFN-γ-treated PTPN2-KD cells compared with respective untreated control shRNA IECs (Fig. 2D, lanes 1 and 2 vs. 4 and 5, respectively). Claudin-2 expression was also confirmed to be higher in PTPN2-KD IECs with or without IFN-γ treatment. Knockdown of STAT1 by siRNA reduced STAT1 phosphorylation and total STAT1 in untreated control shRNA (Fig. 2D, lane 3; Fig. 2E) and PTPN2-KD IECs (Fig. 2D, lane 7; Fig. 2E), as well as IFN-γ–treated control shRNA (Fig. 2D, lane 4; Fig. 2E) and PTPN2-KD (Fig. 2D, lane 8; Fig. 2E) IECs. STAT1 siRNA also reduced claudin-2 expression in untreated PTPN2-KD IECs (Fig. 2D, lane 5 vs. lane 7; Fig. 2F) and following IFN-γ treatment (Fig. 2D, lane 6 vs. lane 8; Fig. 2F). These data demonstrate that STAT1 knockdown reversed the elevated claudin-2 expression observed in PTPN2-KD IECs at rest and following IFN-γ treatment.

STAT1 siRNA reduced junctional membrane-localized claudin-2 and STAT1 nuclear translocation in PTPN2-KD IECs

To determine whether STAT1 regulated claudin-2 localization at cellular junctions, the required site for claudin-2 to functionally modify cation flux, we performed claudin-2 immunolocalization by confocal microscopy. HT-29 Con-shRNA and PTPN2-KD IECs cultured on glass coverslips were transfected with control or STAT1 siRNAs. After 24 h, IFN-γ was added for a period of 24 hours. Cells were fixed with either 4% PFA or 100% methanol and stained for phosphorylated STAT1 (Y701) (p-STAT1) and claudin-2. To confirm decreased p-STAT1 and the effect of STAT1 siRNA in reducing claudin-2 levels in PTPN2-KD IECs (c.f., Fig. 2), we first examined whether nuclear p-STAT1 was elevated in PTPN2-KD IECs and whether this could be reversed by STAT1 siRNA. Nuclear levels of phosphorylated STAT1 (Y701) were elevated in untreated PTPN2-KD IECs versus Con-shRNA IECs (Fig. 3A(i and v); Fig. 3B) and substantially increased by IFN-γ treatment (Fig. 3A(iii and vii); Fig. 3B). As expected, STAT1 siRNA reduced p-STAT1 levels in all conditions (Fig. 3A(ii, iv, vi, viii); Fig. 3B). The intensity of claudin-2 membrane localization was increased in untreated PTPN2-KD compared with untreated Con-shRNA IECs (Fig. 3C(i and v); Fig. 3D). IFN-γ treatment further increased membrane claudin-2 in control and PTPN2-KD IECs (Fig. 3C(iii and vii); Fig. 3D). Claudin-2 staining was partly decreased by STAT1 siRNA transfection in untreated PTPN2-KD IECs, although this just failed to reach statistical significance (Fig. 3C(v and viii); Fig. 3D). However, STAT1 knockdown in PTPN2-deficient cells significantly inhibited the IFN-γ-induced increase in membrane claudin-2 compared with IFN-γ treated Con-shRNA IECs (Fig. 3C(iii and iv); Fig. 3D) and PTPN2-KD IECs transfected with control siRNA (Fig. 3C(vii and viii); Fig. 3D). Overall, these data confirmed that loss of TCPTP promotes claudin-2 expression and

membrane localization through a mechanism involving, at least in part, increased phosphorylation and nuclear localization of STAT1.

Knockdown of STAT1 rescued TER in PTPN2-KD IECs

To determine whether STAT1 siRNA altered the defective barrier function of PTPN2-KD IECs, STAT1 siRNA and control siRNA were transfected into control and PTPN2-KD HT-29 IEC monolayers cultured on Transwells to measure TER. PTPN2-KD IEC monolayers had a lower starting TER than Con-shRNA monolayers, consistent with our previously published data.[34] An siRNA knockdown of STAT1 in PTPN2-KD IECs significantly increased TER over 48 h compared with PTPN2-KD cells transfected with control siRNA (Fig. 4A; $P < 0.01$). By contrast, STAT1 knockdown in control cells did not significantly increase TER above the change observed in control siRNA–transfected Con-shRNA cells. To further confirm the effects of STAT1 knockdown, the percent change in TER due to knockdown of STAT1 in PTPN2-KD cells compared with STAT1 knockdown in Con-shRNA cells revealed that knockdown of STAT1 in PTPN2-KD cells induced a significant increase in TER over Con-shRNA HT-29 cells (Fig. 4B; 29.8 ± 3.9 vs. 13.8 ± 4.2; $P < 0.05$). These data indicate that the underlying decrease in barrier function (TER) in PTPN2-KD IEC monolayers is mediated at least in part by STAT1 and, as indicated by the data presented in Figures 2 and 3, likely occurs through elevated claudin-2 expression and localization to tight junctions.

IFN-′ induces STAT1 binding to the *CLDN2* promoter in PTPN2-KD IECs

We previously reported a STAT-binding site in the *CLDN2* promoter (Fig. 5A).[18] Several transcription factor–binding sites have been identified in the *CLDN2* promoter, including for Caudal-related homeobox 2 (CDX2), which can bind at the CDXB site.[38] Western blot analysis indicated no change in CDX2 expression in PTPN2-KD Caco-2bbe intestinal epithelial cells compared with controls (Fig. 5B). To determine whether STAT1 binds to the *CLDN2* promoter region, we performed chromatin immunoprecipitation of STAT1 and probed for binding of the putative *CLDN2* DNA–binding sequence. Con-shRNA and PTPN2-KD IECs were treated with IFN-γ for 24 h before STAT1 immunoprecipitation of cell lysates. RT-PCR analysis using primers against the STAT-binding region of the *CLDN2* promoter (Fig. 5C; primers listed in Table 1) showed a significant (4.5 ± 1–fold; $P < 0.05$, $n = 3$) increase in binding of STAT1 to the *CLDN2* promoter in PTPN2-KD IECs (Fig. 5D). Confirmation of the specificity of recognition of the STAT-binding site by STAT1 antibody pulldown was made by the lack of detection of AP-1 and NF-κB transcription factor–binding sites in the *CLDN2* promoter as determined by RT-PCR (Fig. 5E). These data indicate that, in TCPTP-deficient IECs, IFN-γ is capable of inducing a significant level of STAT1 binding to the *CLDN2* promoter consistent with the increase in STAT1 nuclear localization observed in Figure 3A (panel vii).

Mutation of the STAT-binding site reverses *CLDN2* promoter induction in PTPN2-KD IECs

To confirm a functional role for TCPTP in restricting *CLDN2* promoter activity, we generated a *CLDN2* promoter–luciferase construct that we transfected into Con-shRNA or PTPN2-KD HT-29 cells. Resting luciferase activity was elevated in untreated PTPN2-KD IECs compared with Con-shRNA HT-29 cells (Fig. 5A). Treatment with IFN-γ (1000 U/mL

(100 ng/mL); 24 h) significantly increased CLDN2–luciferase activity in PTPN2-KD IECs (Fig. 6A). The cumulative effect of TCPTP knockdown and IFN-γ treatment resulted in a 4.7 ± 0.8–fold increase in promoter activity compared with a 2.0 ± 0.5–fold increase following IFN-γ treatment of Con-shRNA cells.

To determine whether the increased *CLDN2* promoter activity in PTPN2-KD cells was due to increased STAT1 binding, we generated single (1M) and triple (3M) point mutations in the STAT-binding site of the *CLDN2* promoter (Fig. 6B and 6C). Both mutants abolished the elevated CLDN2–luciferase activity in PTPN2-KD IECs with or without IFN-γ treatment (Fig. 6D). These data demonstrate that the potentiation of *CLDN2* promoter activity in PTPN2-KD IECs is mediated by STAT binding to the *CLDN2* promoter.

Discussion

Both Crohn's disease (CD) and ulcerative colitis (UC) are characterized by their specific cytokine profile, with elevated levels of IFN-γ predominating in CD.[39] Of the downstream pathways involved in transducing IFN-γ receptor signals, STAT1 and STAT3, members of the STAT family of transcription factors, have perhaps received the most attention with respect to IFN-γ-associated gene transcription.[40] Indeed, upregulation of both STAT1 and STAT3 has been observed in IBD, while both STAT1 and STAT3 have been identified as IBD risk candidate genes.[41–44] We previously identified a STAT-binding motif in the *CLDN2* promoter 261–253 bp upstream of the transcription start site.[18] The identified sequence (5′-TTCCCGGAA-3′, was a positive match for a possible STAT1-binding motif and a confirmed STAT3 binding motif in the human *p21WAF* gene.[45] We therefore set out to determine whether the increase in claudin-2 levels observed in PTPN2-KD IECs was mediated by STAT1 signaling and, secondly, whether this putative STAT-binding motif was responsible for the elevated claudin-2 observed in TCPTP-deficient IECs treated with IFN-γ. Using a novel PTPN2-KD IEC line, we demonstrated that siRNA knockdown of STAT1 partially reduced the elevated claudin-2 expression observed in both untreated and IFN-γ–challenged PTPN2-KD IECs. In agreement with expression data, the elevated levels of claudin-2 in the epithelial membranes of PTPN2-KD IECs were also reduced by STAT1 siRNA. Furthermore, nuclear p-STAT1 was significantly elevated by IFN-γ treatment of PTPN2-KD versus control cells and, as expected, reduced by STAT1 siRNA. These data support our hypothesis that TCPTP restricts claudin-2 expression, at least in part, through its negative regulation of STAT1 signaling. This was also supported by our data indicating that partial siRNA knockdown of STAT1 significantly increased TER in PTPN2-KD HT-29 monolayers. We further demonstrated a physical association between activated STAT1 and the *CLDN2* promoter STAT-binding motif by ChIP analysis (c.f., Fig. 5). To understand the mechanism by which loss of TCPTP expression promoted increased claudin-2 transcription, we generated a *CLDN2* promoter–luciferase construct to show that, under resting and IFN-γ treatment conditions, *CLDN2* promoter activity was increased compared with control-shRNA IECs expressing the same reporter construct. Mutations of the STAT-binding motif completely negated the enhanced *CLDN2* promoter activity in PTPN2-KD IECs.

Cumulatively, we have demonstrated that STAT1 binds to the *CLDN2* promoter to increase *CLDN2* expression via a STAT-binding motif. However, at this time we cannot rule out the

involvement of other STATs in contributing to *CLDN2* promoter activity in TCPTP-deficient IECs. Specifically, we can consider potential roles for STAT3 and STAT5 as TCPTP substrates and mediators of IFN-γ signaling, as well as STAT6, which is an additional substrate of TCPTP and has previously been implicated in promoting claudin-2 levels in response to IL-13 stimulation and in an oxazolone colitis model.[25,46–49] Our data do not entirely align with previous studies that showed that pharmacological inhibition of IFN-γ–stimulated STAT1 tyrosine phosphorylation was unable to alleviate IFN-γ–induced reduction in TER.[50–52] In addition, the same group observed that *STAT1* siRNA did not reverse IFN-′ induction of a drop in TER; however, they did identify an essential role for STAT1 in promoting the capacity of STAT5b to mediate IFN-γ–induced macromolecule (horseradish peroxidase) transepithelial flux across T_{84} colonic epithelial cells. This STAT5b-dependent mechanism involved formation of a complex involving Fyn Src kinase, the G protein adaptor molecule GAB2, and PI3-kinase, thus indicating a requirement for STAT signaling in IFN-γ–stimulated barrier permeability defects associated with macromolecule translocation.[47] Therefore, the potential roles of STAT proteins in the overall regulation of different aspects of epithelial permeability are clearly complex and likely have context-, stimulus-, and cell type–dependent influences. Our findings are also consistent with our earlier observations that, in the context of decreased TCPTP expression, the outcomes of IFN-γ signaling are different than in TCPTP-competent cells.[53] This was perhaps best exemplified by the lack of a significant effect of IFN-γ in stimulating claudin-2 expression in control IECs, which contrasted with the marked upregulation of claudin-2 by IFN-γ in TCPTP-deficient IECs.[18,37] Moreover, IFN-γ–stimulated STAT1 activation was shown to only induce apoptosis of pancreatic β-islet cells when TCPTP levels were knocked down.[54] Thus, loss of TCPTP activity can change the profile of signaling outcomes governed by TCPTP substrates, such as members of the JAK–STAT pathway. Our data show that recruitment of STAT-mediated cytokine signaling is altered in TCPTP-deficient IECs and thus implicate TCPTP activity as a key checkpoint that can restrict the full complement of STAT-mediated transcriptional events.

The *CLDN2* promoter contains a number of transcription factor–binding sites, including sites for NF-κB, AP-1, HNF1A, GATA-4, and the intestine-specific transcription factor CDX2.[27,33,38,55] CDX2 has been identified in a number of studies as a key transcription factor regulating *CLDN2* transcription.[38,56–58] Although investigation of the significance of the STAT-binding site in the *CLDN2* promoter was the focus of this study, we also investigated whether PTPN2-KD IECs exhibited any change in expression of CDX2 and did not see any difference compared with control IECs. While we cannot at this stage rule out possible contributions of TCPTP to regulation of claudin-2 transcription by other transcription factors, particularly when challenged with appropriate cytokines, we have demonstrated a novel role for IFN-γ stimulation of STAT-mediated claudin-2 expression in the setting of reduced TCPTP activity and expression. This has possible implications for IBD, given that subjects harboring loss-of-function mutations in the PTPN2 gene may be further predisposed to increased claudin-2 expression and consequent alterations in intestinal barrier function.

Acknowledgments

This research was supported by NIH R01-DK091281 (DFM), a Senior Research Award from the Crohn's and Colitis Foundation of America (DFM), and a 2016 ASPIRE-Pfizer IBD Research Award (DFM). M.K. helped design experiments, performed experiments, analyzed data, generated figures, and edited the manuscript. D.F.M. conceived and designed research, interpreted results of experiments, obtained funding, and wrote and edited the manuscript.

References

1. Ibarra-Sanchez MJ, Simoncic PD, Nestel FR, et al. The T-cell protein tyrosine phosphatase. Seminars in immunology. 2000; 12:379–386. [PubMed: 10995584]
2. Tiganis T, Bennett AM, Ravichandran KS, et al. Epidermal growth factor receptor and the adaptor protein p52Shc are specific substrates of T-cell protein tyrosine phosphatase. Molecular and cellular biology. 1998; 18:1622–1634. [PubMed: 9488479]
3. Galic S, Hauser C, Kahn BB, et al. Coordinated regulation of insulin signaling by the protein tyrosine phosphatases PTP1B and TCPTP. Molecular and cellular biology. 2005; 25:819–829. [PubMed: 15632081]
4. Zhu W, Mustelin T, David M. Arginine methylation of STAT1 regulates its dephosphorylation by T cell protein tyrosine phosphatase. The Journal of biological chemistry. 2002; 277:35787–35790. [PubMed: 12171910]
5. ten Hoeve J, de Jesus Ibarra-Sanchez M, Fu Y, et al. Identification of a nuclear Stat1 protein tyrosine phosphatase. Molecular and cellular biology. 2002; 22:5662–5668. [PubMed: 12138178]
6. Yamamoto T, Sekine Y, Kashima K, et al. The nuclear isoform of protein-tyrosine phosphatase TC-PTP regulates interleukin-6-mediated signaling pathway through STAT3 dephosphorylation. Biochemical and biophysical research communications. 2002; 297:811–817. [PubMed: 12359225]
7. Bohmer FD, Friedrich K. Protein tyrosine phosphatases as wardens of STAT signaling. JAKSTAT. 2014; 3:e28087. [PubMed: 24778927]
8. Lam MH, Michell BJ, Fodero-Tavoletti MT, et al. Cellular stress regulates the nucleocytoplasmic distribution of the protein-tyrosine phosphatase TCPTP. The Journal of biological chemistry. 2001; 276:37700–37707. [PubMed: 11479308]
9. Bromberg JF, Wrzeszczynska MH, Devgan G, et al. Stat3 as an oncogene. Cell. 1999; 98:295–303. [PubMed: 10458605]
10. Wellcome Trust Case Control, C. Genome-wide association study of 14,000 cases of seven common diseases and 3,000 shared controls. Nature. 2007; 447:661–678. [PubMed: 17554300]
11. Franke A, Balschun T, Karlsen TH, et al. Replication of signals from recent studies of Crohn's disease identifies previously unknown disease loci for ulcerative colitis. Nature genetics. 2008; 40:713–715. [PubMed: 18438405]
12. Todd JA, Walker NM, Cooper JD, et al. Robust associations of four new chromosome regions from genome-wide analyses of type 1 diabetes. Nature genetics. 2007; 39:857–864. [PubMed: 17554260]
13. Smyth DJ, Plagnol V, Walker NM, et al. Shared and distinct genetic variants in type 1 diabetes and celiac disease. The New England journal of medicine. 2008; 359:2767–2777. [PubMed: 19073967]
14. Marcil V, Mack DR, Kumar V, et al. Association between the PTPN2 gene and Crohn's disease: dissection of potential causal variants. Inflammatory bowel diseases. 2013; 19:1149–1155. [PubMed: 23518806]
15. Arrieta MC, Bistritz L, Meddings JB. Alterations in intestinal permeability. Gut. 2006; 55:1512–1520. [PubMed: 16966705]
16. Meddings J. The significance of the gut barrier in disease. Gut. 2008; 57:438–440. [PubMed: 18334657]
17. McCole DF. IBD candidate genes and intestinal barrier regulation. Inflammatory bowel diseases. 2014; 20:1829–1849. [PubMed: 25215613]

18. Scharl M, Paul G, Weber A, et al. Protection of epithelial barrier function by the Crohn's disease associated gene protein tyrosine phosphatase n2. Gastroenterology. 2009; 137:2030–2040. [PubMed: 19818778]
19. Penrose HM, Marchelletta RR, Krishnan M, et al. Spermidine stimulates T cell protein-tyrosine phosphatase-mediated protection of intestinal epithelial barrier function. The Journal of biological chemistry. 2013; 288:32651–32662. [PubMed: 24022492]
20. Bruewer M, Luegering A, Kucharzik T, et al. Proinflammatory cytokines disrupt epithelial barrier function by apoptosis-independent mechanisms. Journal of immunology. 2003; 171:6164–6172.
21. Utech M, Ivanov AI, Samarin SN, et al. Mechanism of IFN-gamma-induced endocytosis of tight junction proteins: myosin II-dependent vacuolarization of the apical plasma membrane. Molecular biology of the cell. 2005; 16:5040–5052. [PubMed: 16055505]
22. Schmitz H, Barmeyer C, Fromm M, et al. Altered tight junction structure contributes to the impaired epithelial barrier function in ulcerative colitis. Gastroenterology. 1999; 116:301–309. [PubMed: 9922310]
23. Heller F, Florian P, Bojarski C, et al. Interleukin-13 is the key effector Th2 cytokine in ulcerative colitis that affects epithelial tight junctions, apoptosis, and cell restitution. Gastroenterology. 2005; 129:550–564. [PubMed: 16083712]
24. Zeissig S, Burgel N, Gunzel D, et al. Changes in expression and distribution of claudin 2, 5 and 8 lead to discontinuous tight junctions and barrier dysfunction in active Crohn's disease. Gut. 2007; 56:61–72. [PubMed: 16822808]
25. Weber CR, Raleigh DR, Su L, et al. Epithelial myosin light chain kinase activation induces mucosal interleukin-13 expression to alter tight junction ion selectivity. The Journal of biological chemistry. 2010; 285:12037–12046. [PubMed: 20177070]
26. Weber CR, Nalle SC, Tretiakova M, et al. Claudin-1 and claudin-2 expression is elevated in inflammatory bowel disease and may contribute to early neoplastic transformation. Lab Invest. 2008; 88:1110–1120. [PubMed: 18711353]
27. Luettig J, Rosenthal R, Barmeyer C, et al. Claudin-2 as a mediator of leaky gut barrier during intestinal inflammation. Tissue barriers. 2015; 3:e977176. [PubMed: 25838982]
28. Yu AS, Cheng MH, Angelow S, et al. Molecular basis for cation selectivity in claudin-2-based paracellular pores: identification of an electrostatic interaction site. J Gen Physiol. 2009; 133:111–127. [PubMed: 19114638]
29. Van Itallie CM, Holmes J, Bridges A, et al. The density of small tight junction pores varies among cell types and is increased by expression of claudin-2. Journal of cell science. 2008; 121:298–305. [PubMed: 18198187]
30. Weber CR, Liang GH, Wang Y, et al. Claudin-2-dependent paracellular channels are dynamically gated. Elife. 2015; 4:e09906. [PubMed: 26568313]
31. Rosenthal R, Milatz S, Krug SM, et al. Claudin-2, a component of the tight junction, forms a paracellular water channel. Journal of cell science. 2010; 123:1913–1921. [PubMed: 20460438]
32. Gunzel D, Fromm M. Claudins and other tight junction proteins. Comprehensive Physiology. 2012; 2:1819–1852. [PubMed: 23723025]
33. Gunzel D, Yu AS. Claudins and the modulation of tight junction permeability. Physiological reviews. 2013; 93:525–569. [PubMed: 23589827]
34. Krishnan M, Penrose HM, Shah NN, et al. VSL#3 Probiotic Stimulates T-cell Protein Tyrosine Phosphatase-mediated Recovery of IFN-gamma-induced Intestinal Epithelial Barrier Defects. Inflammatory bowel diseases. 2016; 22:2811–2823. [PubMed: 27824650]
35. Livak KJ, Schmittgen TD. Analysis of relative gene expression data using real-time quantitative PCR and the 2(−Delta Delta C(T)) Method. Methods. 2001; 25:402–408. [PubMed: 11846609]
36. Stuart RO, Sun A, Panichas M, et al. Critical role for intracellular calcium in tight junction biogenesis. J Cell Physiol. 1994; 159:423–433. [PubMed: 8188760]
37. McCole DF. Regulation of epithelial barrier function by the inflammatory bowel disease candidate gene, PTPN2. Annals of the New York Academy of Sciences. 2012; 1257:108–114. [PubMed: 22671596]
38. Sakaguchi T, Gu X, Golden HM, et al. Cloning of the human claudin-2 5′-flanking region revealed a TATA-less promoter with conserved binding sites in mouse and human for caudal-related

homeodomain proteins and hepatocyte nuclear factor-1alpha. The Journal of biological chemistry. 2002; 277:21361–21370. [PubMed: 11934881]

39. Sasaki T, Hiwatashi N, Yamazaki H, et al. The role of interferon gamma in the pathogenesis of Crohn's disease. Gastroenterologia Japonica. 1992; 27:29–36. [PubMed: 1555746]
40. Stark GR I, Kerr M, Williams BR, et al. How cells respond to interferons. Annual review of biochemistry. 1998; 67:227–264.
41. Schreiber S, Rosenstiel P, Hampe J, et al. Activation of signal transducer and activator of transcription (STAT) 1 in human chronic inflammatory bowel disease. Gut. 2002; 51:379–385. [PubMed: 12171960]
42. Mudter J, Weigmann B, Bartsch B, et al. Activation pattern of signal transducers and activators of transcription (STAT) factors in inflammatory bowel diseases. The American journal of gastroenterology. 2005; 100:64–72. [PubMed: 15654782]
43. Wu F, Dassopoulos T, Cope L, et al. Genome-wide gene expression differences in Crohn's disease and ulcerative colitis from endoscopic pinch biopsies: insights into distinctive pathogenesis. Inflammatory bowel diseases. 2007; 13:807–821. [PubMed: 17262812]
44. Jostins L, Ripke S, Weersma RK, et al. Host-microbe interactions have shaped the genetic architecture of inflammatory bowel disease. Nature. 2012; 491:119–124. [PubMed: 23128233]
45. Ehret GB, Reichenbach P, Schindler U, et al. DNA binding specificity of different STAT proteins. Comparison of in vitro specificity with natural target sites. The Journal of biological chemistry. 2001; 276:6675–6688. [PubMed: 11053426]
46. Lu X, Chen J, Sasmono RT, et al. T-cell protein tyrosine phosphatase, distinctively expressed in activated-B-cell-like diffuse large B-cell lymphomas, is the nuclear phosphatase of STAT6. Molecular and cellular biology. 2007; 27:2166–2179. [PubMed: 17210636]
47. Smyth D, Phan V, Wang A, et al. Interferon-gamma-induced increases in intestinal epithelial macromolecular permeability requires the Src kinase Fyn. Lab Invest. 2011; 91:764–777. [PubMed: 21321534]
48. Rosen MJ, Frey MR, Washington MK, et al. STAT6 activation in ulcerative colitis: a new target for prevention of IL-13-induced colon epithelial cell dysfunction. Inflammatory bowel diseases. 2011; 17:2224–2234. [PubMed: 21308881]
49. Rosen MJ, Chaturvedi R, Washington MK, et al. STAT6 deficiency ameliorates severity of oxazolone colitis by decreasing expression of claudin-2 and Th2-inducing cytokines. Journal of immunology. 2013; 190:1849–1858.
50. McKay DM, Botelho F, Ceponis PJ, et al. Superantigen immune stimulation activates epithelial STAT1 and PI 3-K: PI 3-K regulation of permeability. American journal of physiology Gastrointestinal and liver physiology. 2000; 279:G1094–1103. [PubMed: 11053007]
51. Watson JL, Ansari S, Cameron H, et al. Green tea polyphenol (−)-epigallocatechin gallate blocks epithelial barrier dysfunction provoked by IFN-gamma but not by IL-4. American journal of physiology. 2004; 287:G954–961. [PubMed: 15231486]
52. McKay DM, Watson JL, Wang A, et al. Phosphatidylinositol 3′-kinase is a critical mediator of interferon-gamma-induced increases in enteric epithelial permeability. The Journal of pharmacology and experimental therapeutics. 2007; 320:1013–1022. [PubMed: 17178936]
53. Scharl M, Rudenko I, McCole DF. Loss of protein tyrosine phosphatase N2 potentiates epidermal growth factor suppression of intestinal epithelial chloride secretion. American journal of physiology Gastrointestinal and liver physiology. 2010; 299:G935–945. [PubMed: 20689057]
54. Moore F, Colli ML, Cnop M, et al. PTPN2, a candidate gene for type 1 diabetes, modulates interferon-gamma-induced pancreatic beta-cell apoptosis. Diabetes. 2009; 58:1283–1291. [PubMed: 19336676]
55. Escaffit F, Boudreau F, Beaulieu JF. Differential expression of claudin-2 along the human intestine: Implication of GATA-4 in the maintenance of claudin-2 in differentiating cells. J Cell Physiol. 2005; 203:15–26. [PubMed: 15389642]
56. Sakamoto H, Mutoh H, Sugano K. Expression of Claudin-2 in intestinal metaplastic mucosa of Cdx2-transgenic mouse stomach. Scandinavian journal of gastroenterology. 2010; 45:1273–1280. [PubMed: 20602571]

57. Suzuki T, Yoshinaga N, Tanabe S. Interleukin-6 (IL-6) regulates claudin-2 expression and tight junction permeability in intestinal epithelium. The Journal of biological chemistry. 2011; 286:31263–31271. [PubMed: 21771795]

58. Song X, Chen HX, Wang XY, et al. H. pylori-encoded CagA disrupts tight junctions and induces invasiveness of AGS gastric carcinoma cells via Cdx2-dependent targeting of Claudin-2. Cell Immunol. 2013; 286:22–30. [PubMed: 24287273]

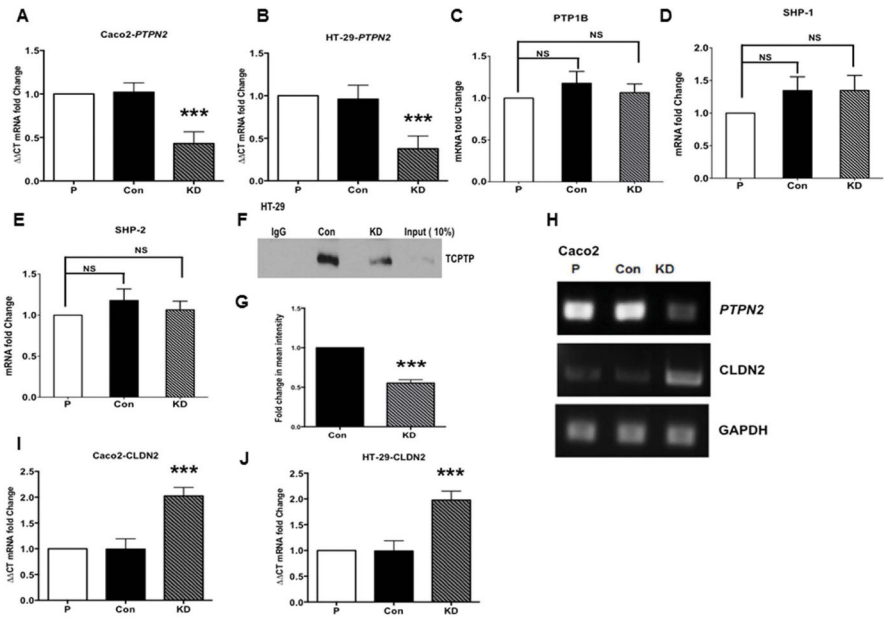

Figure 1.

Stable TCPTP knockdown increases intestinal epithelial claudin-2 transcription. *PTPN2*-shRNA stable knockdown of PTPN2 in Caco-2bbe and HT-29 IEC was achieved using a lentiviral-transfected shRNA (KD). Control (scrambled) shRNA–transfected cells and parental Caco-2bbe and HT-29 cells were also used to quantify *PTPN2*mRNA levels. (A and B) PTPN2-KD cells (KD) showed a significant reduction in TCPTP mRNA relative to parental (P) cell lines (data expressed as ΔΔCT mRNA fold change from parental cell line; $n = 3$) while Con-shRNA transfected cells (Con) showed no difference compared with parental Caco-2bbe or HT-29 cells. (C, D, and E) RT-PCR analysis of mRNA levels for *PTP1B*, *SHP-1*, and *SHP2* showed no difference in PTPN2-KD HT-29 IECs compared with Con-shRNA or parental cells ($n = 3$). (F and G) Con-shRNA and PTPN2-KD cells were lysed with RIPA buffer and immunoprecipitated. TCPTP was analyzed by western blotting to confirm knockdown of TCPTP protein in PTPN2-KD cells (expressed as fold change vs. Con-shRNA levels; $n = 3$). (H) *PTPN2* and *CLDN2* mRNA levels in parental, Con-shRNA, and PTPN2-KD Caco-2bbe cells were determined by RT-PCR. GAPDH was used as a loading control. mRNA quantification by qPCR confirmed a significant increase in *CLDN2* mRNA in (I) Caco-2bbe and (J) HT-29 PTPN2-KD cells relative to parental controls ($n = 3$). Statistical significance was calculated using one-way analysis of variance followed by Student–Newman–Keuls post-test. *** $P < 0.001$; ns, non-significant.

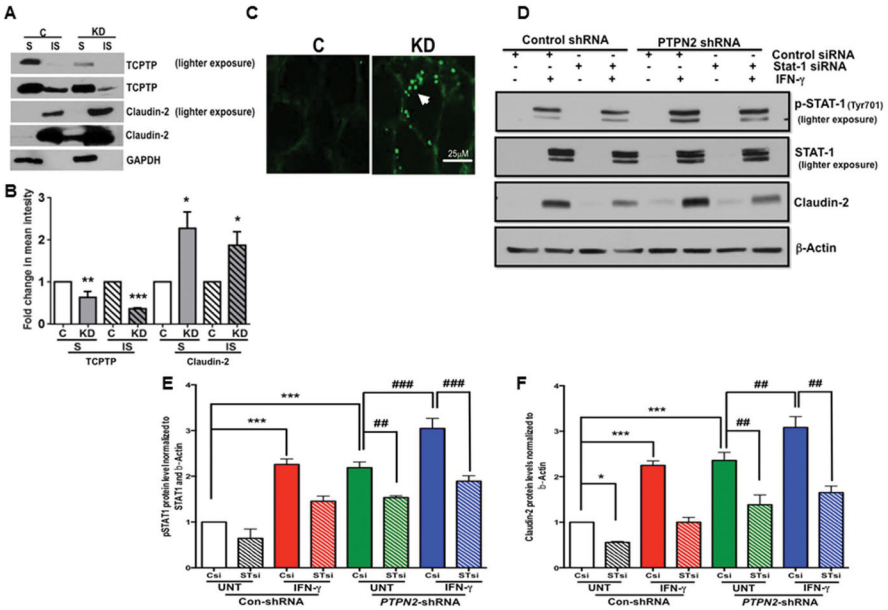

Figure 2.

Increased claudin-2 protein in TCPTP-deficient IECs is alleviated by STAT1 knockdown. (A and B) Soluble and insoluble fractions of HT-29 cell lysates were probed by western blotting to confirm significant knockdown of TCPTP in PTPN2-KD cells in both cytosolic and membrane cell compartments ($n = 3$). Claudin-2 levels were significantly increased in both compartments ($n = 3$). (C) Immunofluorescence staining for claudin-2 (indicated by arrowhead) in Con-shRNA and PTPN2-KD IECs grown on glass coverslips for 3 days (representative of three separate experiments). (D) Con-shRNA and PTPN2-KD HT-29 IEC were transfected with scrambled control siRNA (Csi) or STAT1 siRNA (STsi) and grown on plastic for 24 hours. Cells were treated with IFN-γ (1000 U/mL (100 ng/mL)) or control media (U) for 24 h before whole-cell lysis, western blotting, and densitometric analysis. (E) Phosphorylated STAT1 levels relative to total STAT1 were quantified by densitometry and normalized to β-actin ($n = 5$). (F) Claudin-2 protein levels were quantified by densitometry and normalized to β-actin ($n = 5$). Statistical significance was calculated using one-way analysis of variance followed by Student–Newman–Keuls post-test. * $P < 0.05$, ** $P < 0.01$, *** $P < 0.001$ vs. Con-shRNA in panel B; vs. C-Csi-U in panels E and F. $^{\#\#}$ $P < 0.01$, $^{\#\#\#}$ $P < 0.001$ vs. KD-Csi-U.

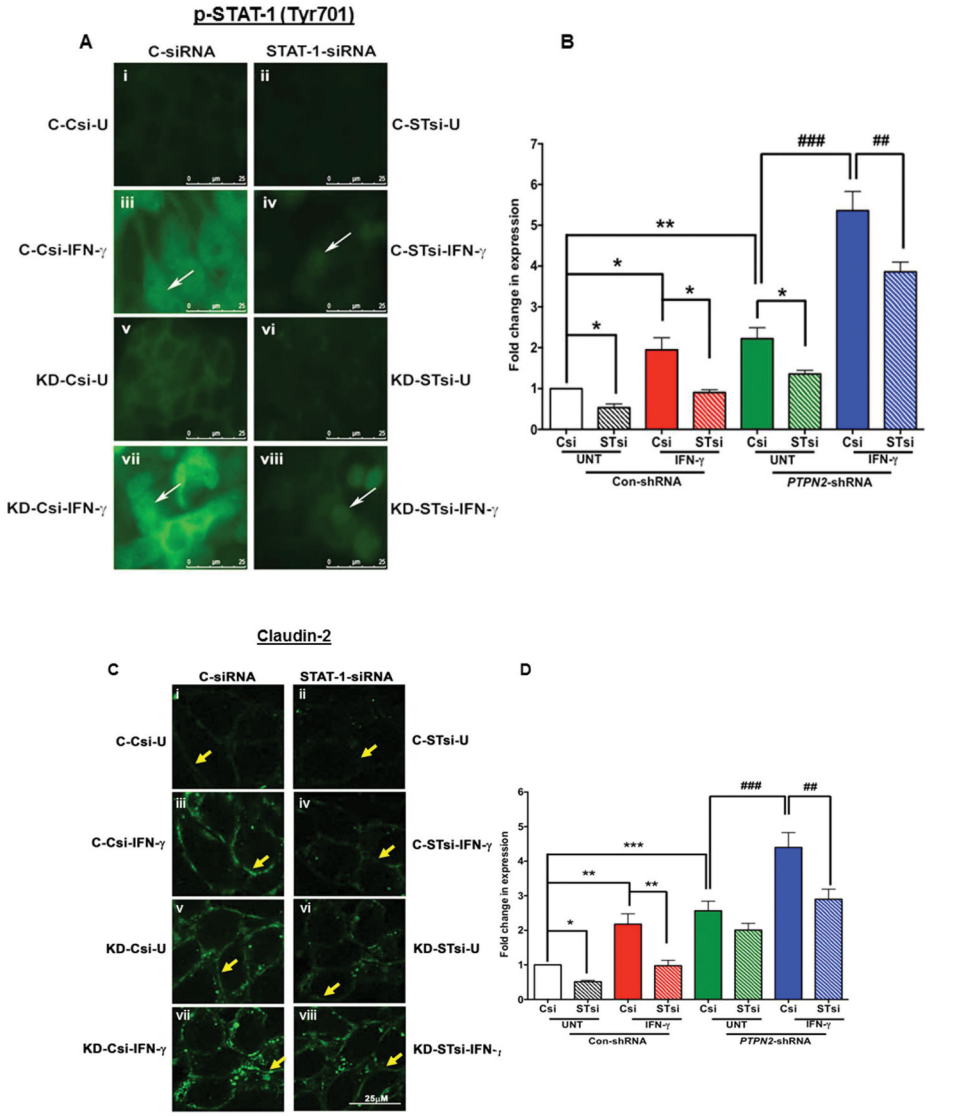

Figure 3.

STAT1 knockdown reduces junctional claudin-2 levels and nuclear translocation of activated STAT1 in PTPN2-KD cells. Control shRNA (C−) or PTPN2-KD (KD−) HT-29 IECs were transfected with scrambled control siRNA (Csi) or STAT1 siRNA (STsi) and grown on coverslips for 24 hours. Cells were treated with IFN-γ or control media (U) for 24 h before fixation with either methanol or 4% PFA. Staining and immunofluorescence quantification for (A and B) p-STAT1 ($n = 3$) and (C and D) claudin-2 ($n = 3$) was performed. Nuclear p-STAT1 is indicated by white arrows. Membrane localized claudin-2 is indicated by yellow arrows. * $P < 0.05$, ** $P < 0.01$, vs. Con-shRNA–CSi-U; $^{\#\#}$, $P < 0.01$ vs. KD-Csi-U.

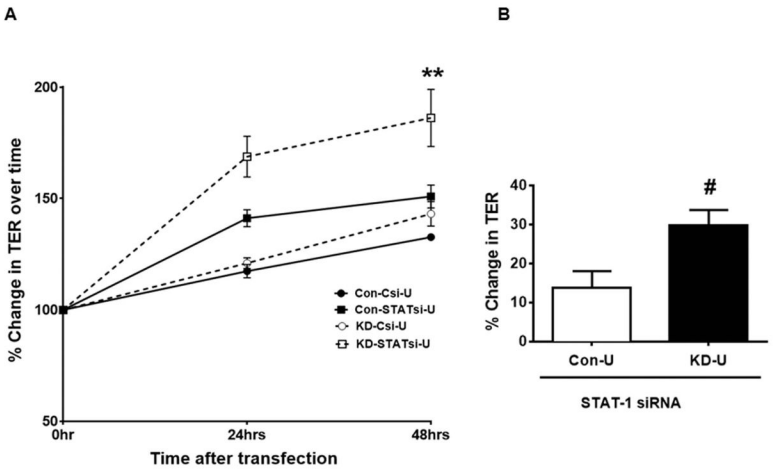

Figure 4.

STAT1 knockdown alleviates the TER defect in PTPN2-KD IEC monolayers. Control shRNA (Con−) or PTPN2-KD (KD−) HT-29 IECs were grown on Transwells for 8 days before transfection with scrambled control siRNA (Csi) or STAT1 siRNA (STATsi). (A) TER ($\Omega \cdot cm^2$) was measured at 0, 24, and 48 h posttransfection, and data were expressed as the percent change in TER over time to correct for the lower resting TER in PTPN2-KD polarized monolayers. (B) The change in TER due to knockdown of STAT1 in Con-shRNA versus PTPN2-KD IEC monolayers was calculated. ** $P < 0.01$, Con-STATsi-U versus KD-STsi-U; $^{\#}$ $P < 0.05$ Con-U versus KD-U; $n = 3$).

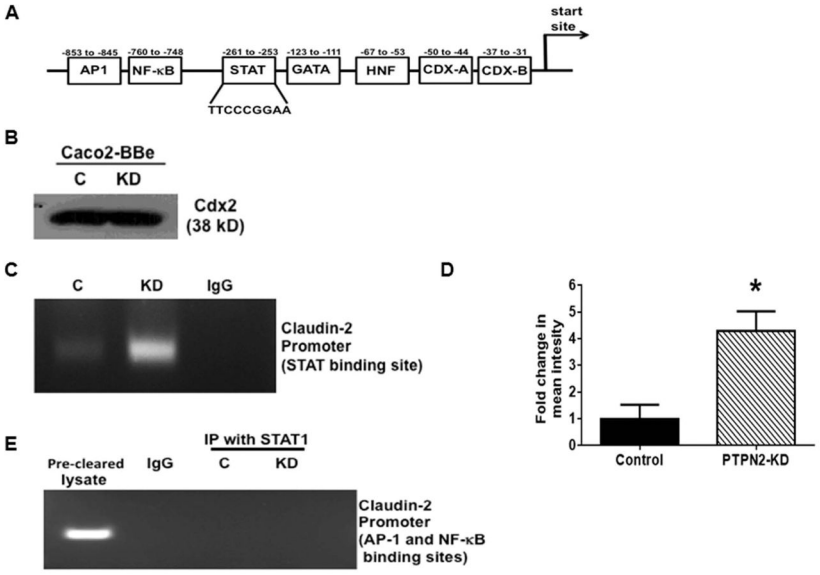

Figure 5.

TCPTP knockdown promotes STAT1 binding to the *CLDN2* promoter. (A) Transcription factor–binding sites in the *CLDN2* promoter, with the STAT-binding site highlighted. (B) Whole-cell lysates from Con-shRNA and PTPN2-KD HT-29 cells were probed by western blotting for the transcription factor CDX2 ($n = 3$). (C) A chromatin immunoprecipitation assay was performed by immunoprecipitating STAT1 from Con-shRNA and PTPN2-KD cells and performing PCR to identify the *CLDN2* promoter STAT-binding sequence. IgG was used as a negative control to confirm specificity of the anti-STAT1 antibody immunoprecipitation. (D) Quantification of PCR data expressed as change in mean intensity. Statistical significance was calculated using unpaired Student's *t*-tests. (E) Chromatin immunoprecipitation assay was performed by immunoprecipitating STAT1 from Con-shRNA and PTPN2-KD cells and performing PCR to identify the *CLDN2* promoter AP-1– and NF-κB–binding sequences. IgG was used as a negative control. * $P < 0.05$; $n = 3$.

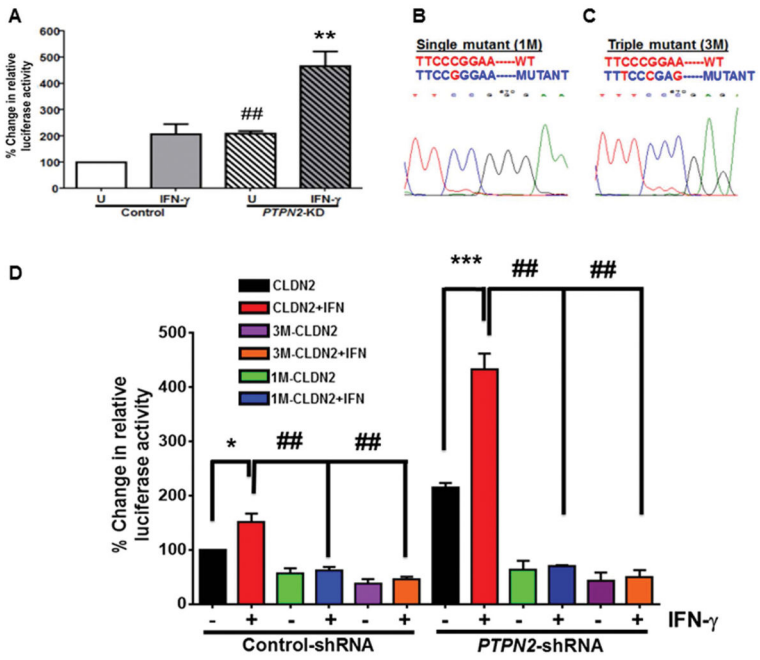

Figure 6.

Increased *CLDN2* promoter activity in TCPTP-deficient cells is dependent on STAT. (A) A *CLDN2* promoter–luciferase construct (1 kb) was generated and expressed in Con-shRNA and PTPN2-KD HT-29 cells. Cells were treated with IFN-γ (1000 U/mL (100 ng/mL)) or media for 24 h and then lysed. Luciferase–promoter activity data were expressed as fold change in intensity relative to luciferase activity in Con-shRNA cells ($n = 3$). (B and C) Schematic and sequence analysis confirmation of the single (1M) and triple (3M) mutations of the STAT-binding site in the *CLDN2* promoter. (D) *CLDN2* promoter–luciferase activity was measured in Con-shRNA and PTPN2-KD HT-29 cells expressing full-length single-mutant (1M) and triple-mutant (3M) *CLDN2* promoter constructs. Statistical significance was calculated using one-way analysis of variance followed by Student–Newman–Keuls post-test. * $P < 0.05$ and *** $P < 0.001$ vs. untreated full-length reporter; $^{\#\#}$ $P < 0.01$ vs. IFN-γ–treated full-length reporter; $n = 3$.

Table 1

Real-time qPCR primer sequences

Symbol	Primer	Sequence (5′–3′)
hPTPN2	Sense	CAGCCGCTGTACTTGGAAATTCG
	Antisense	ATGTGTTAGGAAGTGGACCCTGTG
hGAPDH	Sense	AGATCCCTCCAAAATCAAGTGG
	Antisense	GGCAGAGATGATGACCCTTTT
hCLDN2	Sense	GCATGAGATGCACAGTCTTC
	Antisense	AGGATCCCATGAAGATTCCAGG
ChIP (STAT-binding site)	Sense	GCCTTGGAGACTAGCACTTGAG
	Antisense	CACATGCCTTAGGTTGGCAG
ChIP (AP-1– and NFκB–binding site)	Sense	TGTGCCCTTGACCCTTAGTG
	Antisense	ATGAGGGAGCACTCTGGAAC
hPTP1B	Sense	TCCACTATACCACATGGCCTGAC
	Antisense	AGCCAGACAGAAGGTTCCAGAC
hSHP-1/PTPN6	Sense	GCACCATCATCCACCTCAAGTAC
	Antisense	TGAGCACAGAAAGCACGAAGTC
hSHP-2/PTPN11	Sense	TACGAGAGAGCCAGAGCCAC
	Antisense	CGTTCTCCTCCACCAACGTC

Table 2

ON-TARGETplus SMARTpool siRNA transfection: target sequences

Symbol	Sequence (5′–3′)	Catalog #	siRNA ID #
hSTAT1	GCACGAUGGGCUCAGCUUU	L-003543-00-0005	J-003543-06
	CUACGAACAUGACCCUAUC		J-003543-07
	GAACCUGACUUCCAUGCGG		J-003543-08
	AGAAAGAGCUUGACAGUAA		J-003543-09
Non-targeting sequence	UGGUUUACAUGUCGACUAA	D-001810-10-05	
	UGGUUUACAUGUUGUGUGA		
	UGGUUUACAUGUUUUCUGA		
	UGGUUUACAUGUUUUCCUA		